INSTITUTO TECNOLÓGICO DE AERONÁUTICA

Pedro Kuntz Puglia

PRIMER VECTOR ANALYSIS OF OPTIMAL IMPULSIVE ORBITAL MANEUVERS UNDER CONSERVATIVE AND NON-CONSERVATIVE MODELS

Final Paper
2025

Course of Aerospace Engineering

Pedro Kuntz Puglia

PRIMER VECTOR ANALYSIS OF OPTIMAL IMPULSIVE ORBITAL MANEUVERS UNDER CONSERVATIVE AND NON-CONSERVATIVE MODELS

Advisor

Prof. Dr. Willer Gomes dos Santos (ITA)

Co-advisor

Prof. Emilien Flayac (ISAE-SUPAERO)

AEROSPACE ENGINEERING

São José dos Campos
Instituto Tecnológico de Aeronáutica

2025

BIBLIOGRAPHIC REFERENCE

PUGLIA, Pedro Kuntz. **Primer Vector Analysis of Optimal Impulsive Orbital Maneuvers Under Conservative and Non-Conservative Models**. 2025. 52f. Final paper (Undergraduation study) – Instituto Tecnológico de Aeronáutica, São José dos Campos.

CESSION OF RIGHTS

PRIMER VECTOR ANALYSIS OF OPTIMAL IMPULSIVE ORBITAL MANEUVERS UNDER CONSERVATIVE AND NON-CONSERVATIVE MODELS

This publication was accepted like Final Work of Undergraduation Study

Pedro Kuntz Puglia
Author

Willer Gomes dos Santos (ITA)
Advisor

Emilien Flayac (ISAE-SUPAERO)
Co-advisor

Profa. Dra. Cristiane Martins
Course Coordinator of Aerospace Engineering

São José dos Campos: junho ??, 2025.

Abstract

This work presents the implementation of an orbital maneuver solver under two-body Keplerian dynamics and impulsive thrust model. The control task consists of finding the trajectory between two given states, in a fixed amount of time, minimizing fuel consumption. Optimal control formalism, in the form of the control Hamiltonian, is applied to the problem to uncover the consacrated primer vector theory, which can inform hyperparameter choice. A Julia interface to the recognized Ipopt solver is used to implement a relaxation method for the optimizer. A Lambert problem solver is used to supply a feasible initial guess to the solver. Finally, the results of direct optimization and primer vector theory are compared to the established Hohmann transfer analytical results to validate the implementation.

List of Figures

List of Tables

List of Abbreviations and Acronyms

LEO	Low Earth Orbit
RAAN	Right ascension of the ascending node
TPBVP	Two Point Boundary Value Problem
PMP	Pontryagin's Minimum Principle
STM	State Transition Matrix
PVTM	Primer Vector Transition Matrix
PVDE	Primer Vector Differential Equation

List of Symbols

$\mathbf{x}$	state vector
$\mathbf{u}$	control vector
$\mathbf{r}$	$\mathbb{R}^3$ position vector
$\mathbf{v}$	$\mathbb{R}^3$ velocity vector
$f(\mathbf{x}, \mathbf{u})$	system dynamics
J	cost function
H	system Hamiltonian
λ	costates or adjoint variables
C^1	Set of continuously differentiable functions
μ	Earth's gravitational parameter
a	Semi-major axis
e	Eccentricity
i	Inclination
Ω	Right ascension of the ascending node (RAAN)
ω	Argument of perigee
θ	True anomaly
E	Eccentric anomaly
J_2	Earth's first non-spherical harmonic geopotential coefficient
ρ	Earth's atmospheric density
$\mathbf{F}$	Satellite's thrust vector
m	Satellite's mass
t_f	Total maneuver time, final time for optimal control scenario
Δv	Impulsive velocity discontinuity
Γ	Acceleration magnitude
$\hat{\mathbf{u}}$	Impulse direction
$\mathbf{0}_3$	Null vector in $\mathbb{R}^3$
$\mathbf{0}_{3\times3}$	Null matrix in $\mathbb{R}^{3\times3}$
$\mathbf{p}$	Primer vector
$g(\mathbf{r})$	Conservative gravitational acceleration field
$\boldsymbol{\Phi}_\delta$	State transition matrix (STM)

$\boldsymbol{\Phi}_p$	Primer vector transition matrix (PVTM)
ϵ	Nonlinear solver constraint violation tolerance
$d(\mathbf{r}, \mathbf{v})$	Non-conservative force, usually meant drag
f_{RK}	System dynamics discretized with RK8
d_c	Coast duration
N	Number of integration steps
$\mathtt{C}$	Coasting arc in maneuver sequence
$\mathtt{I}$	Impulse in maneuver sequence
$\mathcal{S}$	Sequence of impulses and coasts in maneuver
$\mathcal{I}$	Set of indices of impulses in maneuver
$\mathcal{C}$	Set of indices of coasts in maneuver
Δx_f	Error between solved final state and final state of propagating optimized maneuver
L	Length scaling parameter
T	Time scaling parameter
$\mathbb{I}$	Unit interval indicator function
σ_k	Smoothened unit interval indicator function with parameter k

Contents

1 Introduction

Space exploration relies on clever resource management, since satellites have a finite amount of resources (propellant and other consumables) to fulfill their mission. Up to this date, all space hardware is expendable, that is, when the consumables required for mission maintenance are finished, the mission ends, marking the end of the exploitation of a very expensive engineered system. The main consumable aboard a satellite is *propellant*, which is used in the satellite's thrusters to impart changes in its trajectory. Changing a satellite's trajectory requires an *orbital maneuver*, that is, a series of thruster activations that removes the satellite from its initial, natural trajectory and takes it to a final, more desirable orbit. There are many possible maneuvers that lead to the same final orbit, with varying propellant consumptions. Finding the smallest propellant consumption is therefore of great interest, which makes the orbital maneuvering problem an *optimal control* problem.

In practice, the nature of a maneuver greatly depends on the propulsion system on-board. Contrary to science fiction, where spaceships seem to be constantly propelled by their thrusters, real life satellites with chemical thrusters change their courses in discrete moments of maximum thrust application, surrounded by (usually long) coasting periods. This is due to the relatively high power delivered by traditional rocket engines, which can, in the matter of seconds or minutes, greatly alter a satelite's orbit. These moments of propelled flight can, to good approximation, be considered as punctual discontinuities in the satellite's velocity. They are called *impulsive maneuvers*. Certain more modern propulsion systems, such as electric rocket engines, are an exception in that the thrust they provide is quite low, and they operate for extended periods of time. In this case, the propelled arcs are long, and the satellite's motion during propulsion must be taken into account. Despite being more modern, electric propulsion systems are not ubiquitous, and chemical propulsion remains the best solution for many applications.

Impulsive maneuvers are described by the impulse magnitudes and the number of impulses. From the point of view of optimization, handling the number of impulses is a challenge, since it is a discrete parameter that cannot be treated as a variable in standard optimal control tools. In practice, this is a problem: the difference in cost of a 2-impulse maneuver and a 4-impulse maneuver can be dramatic, exceeding for instance the cost to

escape Earth's gravity field, as will be seen in the Results section. This means that this is not just a theoretical problem, but quite a pratical one. Luckily, the theory of optimal control applied to orbital maneuvering offers a tool for helping in the search of the number of impulses: the *primer vector* (CONWAY, 2010).

The reasons for performing an orbital maneuver are many: placing the satellite in the correct orbit at the beginning of its lifetime, placing the satellite in a *graveyard* orbit at the end of lifetime, or applying small corrections along its mission to prevent it from straying too far from the mission's requirements. *Maintenance maneuvers* mitigate external perturbations such as atmospheric drag, Earth's oblateness effects (if undesired), gravitational attraction of celestial bodies, and solar radiation pressure during the mission's lifetime to keep the satellite close to the desired orbit. Their frequency and magnitude vary depending on mission requirements, and in industrial applications, other mission requirements must be taken into account when planning maneuvers. The presence of sensitive sensors that must not be pointed at the Sun, solar panels that must always be illuminated, or events such as observation of a ground target are examples of sources of constraints on when maneuvers can be executed. Those are by far the most common type of maneuver, and a loose, non-exhaustive classification arises naturally.

The simplest type of maneuver is that of *orbit raising*, which consists in bringing the satellite from a (often near-circular) orbit and increasing its semimajor-axis (and thus, its period) until a desired value. This maneuver is commonly found in Low Earth Orbit (LEO) applications, due to the presence of atmospheric drag; notably, it is performed by the Internacional Space Station (ISS) about once a month (NASA, 2009). From a theoretical standpoint, it presents a simple, introductory case, often restricted to two dimensions instead of three. There are plenty of theoretical results about it, most notably the Hohmann transfer (CHOBOTOV, 2002), a two-impulse maneuver which is known to be the two-impulse optimal from a plethora of theoretical tools. Other more elaborate results include the bielliptic transfer (CHOBOTOV, 2002), which can be shown to surpass Hohmann's performance in certain conditions by allowing a third impulse.

A second type of maneuver is a *plane change* maneuver (CURTIS, 2020). Satellites move (approximately) in a plane which contains its position and velocity vectors and the center of Earth. By changing the direction of the velocity, this plane may be change. Common cases include an inclination change during orbital insertion, which may be required if the inclination of the target orbit is different to the latitude of the launch center (CURTIS, 2020). Another type of maneuver is the *phasing* maneuver (CURTIS, 2020). This maneuver consists in changing the position occupied by the satellite within the same orbit at a certain time. This maneuver is very important for *orbital rendez-vous*, where not only it is required that two vessels share the same orbit, but also they must have the same position and velocity at the same time. A notable, recurring example of rendez-vous is that be-

tween the Soyuz capsule and the ISS, which requires agreement of all orbital elements and the correct phasing. This is usually a multi-revolution maneuver but recent advances have greatly reduced the time required for the rendez-vous (PARADISO, 2025). Finally, at the end-of-life, there are legal constraints on where a satelite may be disposed of. NASA LEO missions have a deadline of 25 years for deorbiting into Earth's atmosphere (AERONAU-TICS; ADMINISTRATION, 2021), while GEO satellites are usually placed into a cemetery orbit which does not intersect the highly prized GEO region. As an end-of-life procedure, feasibility is of utmost importance, while ensuring optimality increases the lifespan of the mission.

Of particular interest to Brazil's space program are maneuvers in LEO. The ITASAT-2 project proposes a flight formation of 3 satellites in LEO that must keep precise positions through the usage of chemical thrusters (SATO *et al.*, 2023). While previous work considers relative position control in a small deviations context (FRANCO; SANTOS, 2020), this work shall tackle the full problem of planning generic orbital maneuvers in LEO.

1.1 Problem statement

The central question of this work is how to find the most efficient sequence of impulsive maneuvers that take a satellite from an initial state to a final state in a given amount of time, under perturbed orbital models. The problem's domain is restricted to LEO orbits, and a time horizon of a few revolutions. Here, most efficient is defined as least propellant consumption. No assumption of circular or coplanar orbits, or any other simplifying assumption about initial and final states is allowed in the modelling and algorithms of this work. The work is restricted to finding satisfactory local optima, instead of trying to characterize the global optimum or its lower bounds.

A central topic to be explored is the question of how many impulses are needed for a particular maneuver. This is the most classic question in the field, but still a topic of research (TAHERI; JUNKINS, 2019). This matter shall be explored with primer vector theory (CONWAY, 2010), which is often presented for a two-body orbital model. This theory shall be extended to encompass relevant orbital disturbances in LEO maneuvering scenarios.

The proposed scenarios in this work are a circular-to-circular rendez-vous problem and a non-coplanar rendez-vous in multiple revolutions. The goal is to validate the results under the two body model with the results for the known Hohmann transfer (CURTIS, 2020) and previous results in the primer vector field, as in Luo *et al.* (2010). Then, the same scenarios are to be solved under perturbed orbital models, including oblateness effects and drag, extending the domain of the primer vector method to new models.

1.2 Hypotheses

The impulsive maneuver optimization problem is expected to be reducible to a simple parameter optimization problem where impulse parameters are directly optimized in modern non-linear optimizers with a multiple shooting scheme, which is standard in optimal control and in the field of impulsive maneuvers (BOKELMANN; RUSSELL, 2019). The need for numerical solutions is well established and taken as granted. However, it is expected that many local optima are to be found, due to the non-convex nature of direct optimal control problems and of the domain of the state vector, and the periodic motion of satellites, which makes multi-revolution transfers particularly challenging.

The time of transfer is frequently treated as a fixed input parameter, both in the theory (CONWAY, 2010) and in research (LION; HANDELSMAN, 1968), since it can prevent optimizers from generating infinite-time maneuvers (BOKELMANN; RUSSELL, 2019). The longer the transfer time, the more revolutions around the central body are expected, and the more (small) impulses are expected. The more revolutions are allowed, the more local optima of bad performance are expected, requiring more computational work to arrive at satisfactory solution.

Primer vector theory is expected to be useful for determining how many impulses are necessary, up to the question of whether a solution that satisfies the necessary conditions is actually a satisfactory solution. The problem is known to have many local optima (LUO *et al.*, 2010), but it is expected that primer vector theory will always improve, or maintain performance, of a given suboptimal solution by adding or removing impulses (CONWAY, 2010). That is, primer vector theory should produce a decreasing sequence of costs.

The primer vector literature under the two body model is extensive, with some works applying it to the restricted three body problem (BOKELMANN; RUSSELL, 2019). However, no work was found applying this theory to orbital perturbations in LEO, namely Earth's oblateness effects and atmospheric drag. Therefore, it is expected that some adaptation of the theory is in order to apply the primer vector method to perturbed models.

Finally, due to the existence of many suboptimal solution, and the expected usage of local optimizers, it is expected that solutions will be locally optimal with no guarantee of global optimality. Ensuring global optimality is a much harder problem and, except in particular cases where physical reasoning may give insight, or the mathematical structure of the problem allows for a systematic lower bound estimation.

1.3   Objectives

The objective of this work is to extend to perturbed orbital models the primer vector method for finding the optimal sequence of impulses that transfer a satellite from an arbitrary starting orbit to an arbitrary final orbit, in a given amount of time, and apply it for some practical scenarios. Secondary objectives include:

- Compare maneuvers with known solutions under the standard two body model with their perturbed-model counterparts;

- Describe different methods for calculating the primer vector, and the domain of validity of each one;

- Present a multiple-shooting algorithm for optimizing maneuvers with a fixed number of impulses;

- Discuss the limitations of the presented methods in terms of problem size, numerical accuracy, and solver characteristics.

1.4   Work structure

This work is organized in chapters as follows:

1. **Introduction**, where preliminary contextualization is given;

2. **Theory** and fundamentals, where the mathematical description of the problem is given;

3. **Bibliographic review**, where some previous results in the field are discussed;

4. **Methodology**, where implementation details are given;

5. **Results**, where numerical scenarios exemplify the proposed method, and comparisons with known results are made;

6. **Conclusion**, where the merits and issues of this work are summarized, and future investigations are proposed.

2 Theory and fundamentals

This work relies on optimal control theory and orbital mechanics. Certain tools from optimal control theory are necessary to analyze the conditions for a control trajectory to be the best according to some criterion, and under some mathematical conditions. This theory applies to a wide range of linear and non-linear systems, independently of the specifics of a dynamical system. However, this works focuses its application to one particular system: that of a body gravitationally attracted by a much more massive central body, which is the domain of orbital mechanics. Both theories will be introduced in the following sections.

2.1 Optimal Control

Optimal control is the area of control theory which tries to find the best control action to satisfy some requirements, such as altering a system's state in some desired way. Here, "best" is defined as maximizing or minimizing some performance metric. In practice, and in particular in the scope of this work, this can be interpreted as attaining a target orbit in a certain amount of time, while minimizing fuel consumption.

The mathematical nature of an optimal control problem varies greatly depending on the nature of the system, the requirements, and the objective. Here, a selected subset of this vast theory shall be presented. Suppose a continuous time dynamical system operating on times $t \in [0, t_f]$, where $t_f \in \mathbb{R}$, given by

$$\dot{\mathbf{x}}(t) = f(\mathbf{x}(t), \mathbf{u}(t)) \tag{2.1}$$

where $\mathbf{x}(t) : \mathbb{R} \to \mathbf{x} \subset \mathbb{R}^n$ is the state vector trajectory describing the system state, $\mathbf{u}(t) : \mathbb{R} \to \mathbb{R}^m$ is the control vector trajectory and $f : \mathbb{R}^n \times \mathbb{R}^m \to \mathbb{R}^n$ is the function describing its temporal dynamics. Those functions are supposed to belong to function spaces with certain regularity properties, which will be discussed in Section 2.3.2 in the context of impulsive control.

In addition, the control vector might be subject to some some inequality constraints,

representing for instance saturation of actuators. Therefore, an admissible control set $\mathcal{U}$ is defined by a vector of constraint functions $\mathbf{g}(\mathbf{u})$ as

$$\mathcal{U} = \{\mathbf{u} \in \mathbb{R}^m | \mathbf{g}(\mathbf{u}) \leq 0\} \tag{2.2}$$

where the inequality is understood to hold component-wise.

At the initial time, the system is supposed to be in a given state $\mathbf{x}_i$ such that

$$\mathbf{x}(0) = \mathbf{x}_i. \tag{2.3}$$

At the final time t_f, some components of the final state vector are specified, while others are subject to optimization. Let the index set $\mathcal{K}$ be the set of state variables that are fixed at the final time, such that

$$(\mathbf{x}(t_f))_k = (\mathbf{x}_f)_k, k \in \mathcal{K}, \tag{2.4}$$

where $\mathbf{x}^k$ denotes the k-th component of $\mathbf{x}$, for some given values $\mathbf{x}_f^k$.

To complete the optimal control problem, a performance metric needs to be introduced. In general, any functional of the form $J[\mathbf{x}(t), \mathbf{u}(t)]$ may be taken as this performance metric; however, a common form which shall be adopted in this work, is given by

$$J[\mathbf{x}(t), \mathbf{u}(t)] = h(\mathbf{x}(t_f)) + \int_0^{t_f} L(\mathbf{x}(t), \mathbf{u}(t))dt \tag{2.5}$$

where the functions $h(\mathbf{x})$ and $L(\mathbf{x}, \mathbf{u})$ are respectively called the *terminal cost* and the *temporal cost* functions (BERTSEKAS, 1995).

The optimal control problem is then that of finding a control trajectory $\mathbf{u}(t)$ that minimizes (or maximizes) the performance metric. Here the problem shall be presented as a minimization problem; but the formulation is perfectly analogous for a maximization problem. That said, the complete optimal control problem may be stated as finding the function $\mathbf{u}(t)$ such that (BRYSON; HO, 1975)

$$\mathbf{u}(t) = \arg \min_{\mathbf{u}(t), \mathbf{x}(t)} J[\mathbf{x}(t), \mathbf{u}(t)] \tag{2.6}$$

subject to

$$\dot{\mathbf{x}}(t) = f(\mathbf{x}(t), \mathbf{u}(t)) \tag{2.7}$$

$$\mathbf{x}(0) = \mathbf{x}_i \tag{2.8}$$

$$(\mathbf{x}(t_f))_k = (\mathbf{x}_f)_k, k \in \mathcal{K}. \tag{2.9}$$

In general, this is a very hard problem. The optimization variables $\mathbf{u}$ and $\mathbf{x}$ are infinite dimensional. There are techniques to turn this problem into a simple parameter optimization problem, which are known as *direct methods* (CONWAY, 2010), which shall be discussed later. There are however tools for extracting necessary conditions for the optimal solution of this problem at all points in time. These are known as *indirect methods*.

One of this tools is the Hamiltonian (CONWAY, 2010), a quantity that describes the ensemble of objectives and constraints. It shall be defined for a minimization problem, and maximization problems can be adapted by changing the sign of the performance metric. Given a system of the form in Equation (2.1), constraints in the forms of Equations (2.3) and (2.4), and a cost function in the form (2.5), the Hamiltonian H is defined as (BERTSEKAS, 1995)

$$H(\mathbf{x}(t), \mathbf{u}(t), \lambda(t)) = L(\mathbf{x}, \mathbf{u}) + \lambda(t)^T f(\mathbf{x}, \mathbf{u}) \tag{2.10}$$

for all times t, state and control vectors $\mathbf{x}$ and $\mathbf{u}$ along a trajectory. $\lambda : \mathbb{R} \to \mathbb{R}^n, \lambda \in C^1$ is the costate trajectory, a new set of variables introduced as the continuous-time equivalent of Lagrangian multipliers. These new variables are subject to the adjoint equations

$$\dot{\lambda} = -\left(\frac{\partial H}{\partial \mathbf{x}}\right)^T = -\left(\frac{\partial f}{\partial \mathbf{x}}\right)^T \lambda - \left(\frac{\partial L}{\partial \mathbf{x}}\right)^T \tag{2.11}$$

and boundary conditions (BRYSON; HO, 1975)

$$\lambda^k(t_f) = \frac{\partial h(\mathbf{x}(t_f))}{\partial \mathbf{x}^k}, k \notin \mathcal{K}. \tag{2.12}$$

An important property of the Hamiltonian for fixed-time problems is that its value is constant with respect to time along the optimal trajectory (BERTSEKAS, 1995). For an optimal trajectory $\mathbf{x}^\star(t)$, $\mathbf{u}^\star(t)$, $\lambda^\star(t)$, and some value $C \in \mathbb{R}$,

$$H(\mathbf{x}^\star(t), \mathbf{u}^\star(t), \lambda^\star(t)) = C, \forall t \in [0, t_f]. \tag{2.13}$$

To complete the Hamiltonian approach, Pontryagin's Minimum Principle (PMP) is introduced. It states that a necessary condition for attaining the minimum in Equation (2.6) is that, at all times t, and along the optimal trajectory, (BERTSEKAS, 1995)

$$\mathbf{u}^\star(t) = \arg\min_{\mathbf{u} \in \mathcal{U}} H[\mathbf{x}(t), \mathbf{u}, \lambda(t)]. \tag{2.14}$$

With the control trajectory obtained as a function of $\mathbf{x}(t)$ and $\lambda(t)$ from Equation (2.14), there are 2n variables, the state and costate trajectories, and 2n boundary conditions, the initial states, some final states and some final costates according to

Equations (2.4) and (2.12). Thus, the problem is well-posed and configures a Two Point Boundary Value Problem (TPBVP) (BRYSON; HO, 1975).

It is worth highlighting that in optimal control problems, a hierarchy of solutions exist (ROSS, 2015), shown in Figure 2.1. The least valuable solution is a mere feasible solution, which satisfies the constraints, but is not optimal in any sense. It is enough in some applications, but not in others. Next, local optima have generally lower costs, and are found numerically with nonlinear solvers, but no not necessarily reflect extrema of the original problem. If it can be shown that a local optimum also satisfies the PMP, it comes is inherently a more valuable solution, since it satisfies the necessary conditions to be an extremum of the problem. The most valuable solution type, and the one which is almost impossible to characterize, are global optima, which are guaranteed to have the lowest possible feasible cost for the problem. Finally, lower bound estimations give (infeasible) costs which are guaranteed to be lower than the global optimum, and can be estimated physically (BOKELMANN; RUSSELL, 2019) or mathematically, for instance with sum-of-squares decompositions (LASSERRE, 2009). This work will search for extrema satisfying the PMP.
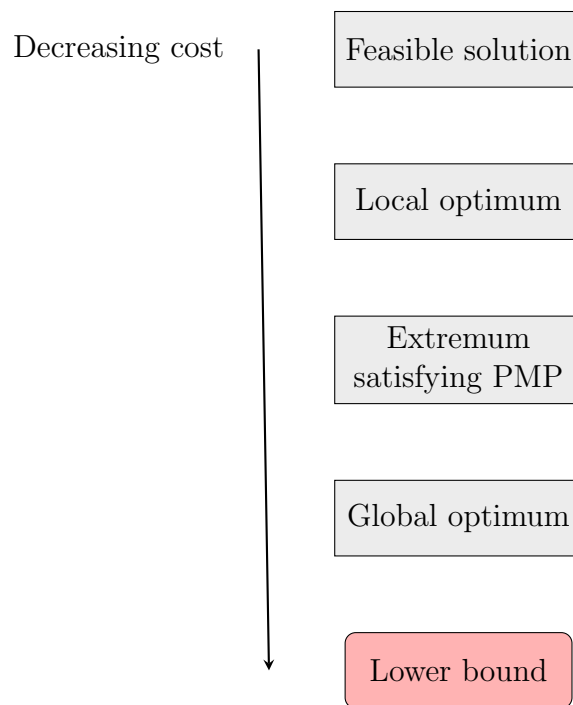

FIGURE 2.1 – Hierarchy of optimal control problem solutions. Adapted from Ross (2015).

TODO: NUMERICAL APPROACH: MULTIPLE SHOOTING

2.2   Orbital Mechanics

Orbital mechanics concerns itself with the motion of bodies in space subject to gravitational and disturbance forces. A variety of models exist, differing in precision and availability of analytical tools. The simpler the model, the more analytical tools are available, and the smaller the precision. The simplest model of all, and the basis for all others, is the two body problem, where a central massive body is supposed to be stationary while a moving satellite is subject to its gravitational attraction, also known as Keplerian motion.

2.2.1   Two Body Motion

Let $\mathbf{r}$ be the 3-dimensional position of a satellite, and μ the gravitational parameter of the central body. The dynamics of the satellite's position are given by (CURTIS, 2020)

$$\ddot{\mathbf{r}} = g(\mathbf{r}) = -\frac{\mu}{\|\mathbf{r}\|^3}\mathbf{r}, \tag{2.15}$$

where $g(\mathbf{r})$ represents the gravitational acceleration field, thus configuring a 6-dimensional state vector $\mathbf{x} = \begin{bmatrix} \mathbf{r}^T & \mathbf{v}^T \end{bmatrix}^T$, where $\mathbf{v}$ is the satellite's velocity. The system contains a singularity at the states with $\|\mathbf{r}\| = 0$, which configures a non-convex domain. In practice, this point is rarely encountered as it lies inside of the central body, thus far from the regions of interest. It is proven that no analytical solution exists for this differential equation; however, much is known about its solutions.

In this model, the possible trajectories are known to be conics, and therefore restricted to a plane. For bound satellites, that is, those in orbit around the central body, this trajectory is an ellipse where the central body lies on one of its foci. Mathematically, a "bound" satellite is one whose specific energy (mechanical energy over mass of the satellite), given by (CURTIS, 2020)

$$\epsilon = -\frac{\mu}{\|\mathbf{r}\|} + \frac{\mathbf{v}^2}{2}, \tag{2.16}$$

is negative. The trajectory is closed, and the movement is periodic with period (CURTIS, 2020)

$$T = 2\pi\sqrt{\frac{a^3}{\mu}} \tag{2.17}$$

where a is the semi-major axis of the ellipse.

In this case, an alternative state vector may be introduced in the form of the Keplerian elements. These are (CURTIS, 2020):

- a: semi-major axis of the ellipse;

- e: excentricity of the ellipse;

- i: inclination of the orbit's plane with respect to the equatorial plane;

- Ω: right ascension of the ascending node, that is, angle between the vernal equinox direction and the direction where the satellite crosses the equatorial plane from South to North;

- ω: argument of perigee, or angle, in the plane of the orbit, between the ascending node and the perigee (point of smallest distance to the central body);

- θ: true anomaly, or angle between the perigee and the current position of the satellite.

These elements are related to the Cartesian state vector through the geometric description of a point on an ellipse, rotated through the Euler angles Ω, i, ω (CURTIS, 2020).

In this formulation, only the true anomaly is a function of time, all other elements being constant. The true anomaly can be related to time implictly through two other quantities, the mean anomaly M and the excentric anomaly E (CURTIS, 2020):

$$M = 2\pi \frac{t - t_p}{T} \tag{2.18}$$

$$E - e\sin E = M \tag{2.19}$$

$$\tan\frac{\theta}{2} = \sqrt{\frac{1+e}{1-e}} \tan\frac{E}{2} \tag{2.20}$$

where t_p is the time of the last perigee passage. By computing the mean anomalies in an initial and a final time, and solving the notorious Kepler's Equation (2.19), and finally finding a suitable true anomaly with Equation (2.20), a semi-analytical temporal solution can be found. The process of finding the position of a satellite in the future is called *orbit propagation*. Define an orbit propagator as a funcion $p_o(\mathbf{x}_i, t)$ such that

$$\mathbf{x}_f = p_o(\mathbf{x}_i, t) \tag{2.21}$$

where $\mathbf{x}_f$ is the satellite's final state after a time t, with initial state $\mathbf{x}_i$.

2.2.2   Orbital Perturbations

The two body model is an idealized model amenable to analytical solutions, which neglects many real world phenomena. In LEO, the most important perturbations are oblateness effects (J2) and atmospheric drag (CURTIS, 2020), which are introduced ahead.

2.2.2.1   Oblateness effects

The Earth being an oblate spheroid, its gravity field is not perfectly central, neither does it behave like the inverse square law predicted by the two body model. Instead, the Earth's geopotential is modeled as a point mass potential plus spherical harmonics terms with coefficients subject to empirical fitting. The biggest non-sphericity of Earth is its oblateness, the increased width at the Equator. This effect is described by the coefficient J_2, which causes a perturbing acceleration $\mathbf{a}_{J2}$ given by

$$\mathbf{a}_{J2} = \frac{3 J_2 \mu R^2}{2 r^4} \begin{bmatrix} \frac{x}{r} \left(5 \frac{z^2}{r^2} - 1 \right) \\ \frac{y}{r} \left(5 \frac{z^2}{r^2} - 1 \right) \\ \frac{z}{r} \left(5 \frac{z^2}{r^2} - 3 \right) \end{bmatrix}, \tag{2.22}$$

where R is Earth's Equatorial radius.

Thus, this model's dynamics can be expressed solely as a function of the position, since it is a conservative model:

$$\ddot{\mathbf{r}} = g_{J2}(\mathbf{r}) = -\frac{\mu}{r^3} \mathbf{r} + \mathbf{a}_{J2}. \tag{2.23}$$

2.2.2.2   Atmospheric Drag

Atmospheric drag affects satellites in LEO by generating a force opposed to the relative velocity of the satellite w.r.t. the Earth's atmosphere, which rotates with it. The drag force is proportional to atmospheric density $\rho(r)$, as a function of the satellite's distance to Earth. Modelling this dependence is not a trivial task, with accurate models taking solar activity and Earth's temperature into account. A simple model is given by the US Standard Atmosphere 1976, which gives empirical coefficients ρ_i and H_i, valid for height intervals $[h_i, h_i + 1]$, for $i = 1, \ldots, 28$. Then, atmospheric density is given piecewise by

$$\rho(r) = \rho_i \exp\left(-\frac{(r - (h_i + R))}{H_i} \right), \tag{2.24}$$

where i is such that $h_i \leq r - R \leq h_{i+1}$. The satellite is parameterized by a reference surface S, drag coefficient C_D and mass m. Considering that the Earth rotates with

angular velocity ω_E, the relative velocity of the satellite w.r.t. the atmosphere is given by

$$\mathbf{v}_r = \mathbf{v} - (\omega_E \hat{\mathbf{z}}) \times \mathbf{r}. \tag{2.25}$$

Finally, the acceleration due to drag $\mathbf{a}_D$ is given by

$$\mathbf{a}_D = -\frac{1}{2}\rho(r)\frac{SC_D}{m}\|\mathbf{v}_r\|\mathbf{v}_r, \tag{2.26}$$

which can be added as a perturbing non-conservative acceleration to the model.

2.2.3 Lambert's Problem

An important problem in orbital mechanics is that of the determination of the initial and final velocities of a satellite that passes through two points in space $\mathbf{r}_1$ and $\mathbf{r}_2$ with a time interval Δt in between, as illustrated in Figure 2.2. This problem first arose in the field of orbit determination but also finds application in the context of orbital maneuvers. Namely, Lambert's Problem seeks to find a feasible solution to a TPBVP, which is of interest to the optimal control TPBVP.
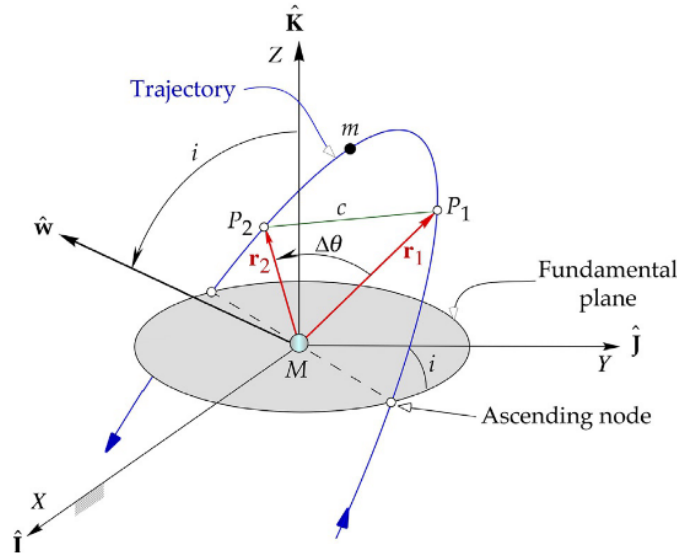
FIGURE 2.2 – Lambert problem illustration showing initial and final positions $\mathbf{r}_1$ and $\mathbf{r}_2$ and the (computed) trajectory that connects them in time Δt. Source: (CURTIS, 2020)

This problem suffers from a physical indetermination in the case of collinear r_1 and r_2: the plane of the orbit is indeterminate. In this case, one can find many feasible solutions but determining exact velocities requires extra information about the plane of the orbit.

In general, this problem can have multiple solutions, corresponding to prograde and retrograde trajectories, with less than one or multiple revolutions. The resulting orbit

can, in general, be elliptic, parabolic or hyperbolic. Handling this variety of solution types is not simple. A simple formulation which does not handle multiple revolutions nor the indetermination mentioned can be built with universal variables (CURTIS, 2020). Multiple revolutions and finding the radial and tangent components of the velocity in the indeterminate case can be handled with more complex algorithms (SUKHANOV, 2010). A generic, Cartesian coordinates-based algorithm is also possible, as will be discussed in Chapter 4.

2.2.4   State Transition Matrix

It is sometimes useful to characterize how the solution of an ODE depends on its initial condition. For the solution $\mathbf{x}(t) \in \mathbb{R}^n$ of the dynamical system $\dot{\mathbf{x}} = f(\mathbf{x})$ with initial condition $\mathbf{x}_0$, this is mathematically described by the state transition matrix (STM) $\Phi_\delta(t) \in \mathbb{R}^{n \times n}$:

$$\Phi_\delta(t) = \frac{\partial \mathbf{x}(t)}{\mathbf{x}_0}. \tag{2.27}$$

In general, this matrix is subject to the initial value problem (MONTENBRUCK; GILL, 2000)

$$\begin{cases} \dot{\Phi}_\delta(t) = \frac{\partial f(\mathbf{x}(t))}{\partial x(t)} \Phi_\delta(t) \\ \Phi_\delta(0) = \mathbf{I}_n \end{cases} \tag{2.28}$$

with n^2 variables and initial conditions.

In particular, for a double-integrator system with position $\mathbf{r}$ and velocity $\mathbf{v}$ in the state vector described by

$$\dot{\mathbf{x}} = \begin{bmatrix} \dot{\mathbf{r}} \\ \dot{\mathbf{v}} \end{bmatrix} = \begin{bmatrix} \mathbf{v} \\ \mathbf{a}(\mathbf{r}, \mathbf{v}) \end{bmatrix}, \tag{2.29}$$

the STM equation can be expanded to

$$\dot{\Phi}_\delta(t) = \begin{bmatrix} \mathbf{0}_{3 \times 3} & \mathbf{I}_3 \\ \frac{\partial \mathbf{a}(\mathbf{r}(t), \mathbf{v}(t))}{\partial \mathbf{r}} & \frac{\partial \mathbf{a}(\mathbf{r}(t), \mathbf{v}(t))}{\partial \mathbf{v}} \end{bmatrix} \Phi_\delta(t) = A_\delta(\mathbf{r}(t), \mathbf{v}(t))\Phi_\delta(t), \tag{2.30}$$

where $A_\delta(\mathbf{r}(t), \mathbf{v}(t))$ is defined to be matrix coefficient of the STM in its differential equation. Note also that any vector ODE with state $\mathbf{z}(t) \in \mathbb{R}^n$ subject to

$$\dot{\mathbf{z}}(t) = A_\delta(\mathbf{r}(t), \mathbf{v}(t))\mathbf{z}(t), \tag{2.31}$$

its solution is given in terms of the initial condition $\mathbf{z}_0$ and the STM:

$$\mathbf{z}(t) = \Phi_\delta(t)\mathbf{z}_0. \tag{2.32}$$

For a two-body model, an analytical expression for the STM exists, given for instance in Montenbruck e Gill (2000) and GLANDORF (1969).

2.3   Orbital Maneuvers

When a satellite is able to maneuver, the Keplerian dynamics of Equation (2.15) need to be augmented with the thrust control vector $\mathbf{F}$, which applies a propulsion force on the satellite. Supposing that m is the total current mass of the spacecraft, which in general is a seventh state variable (in addition to orbital state variables), the dynamics are given by

$$\ddot{\mathbf{r}} = -\frac{\mu}{\|\mathbf{r}\|^3}\mathbf{r} + \frac{\mathbf{F}}{m}. \tag{2.33}$$

The generation of thrust $\mathbf{F}$ is tied to the consumption of propellant, according to some propulsion model. Three main models exist. The first is the constant specific impulse continuous (as opposed to instantaneous) thrust model, adequate for chemical engines. The second is the impulsive thrust model, the limiting case of the previous model where a burn is considered to happen instantly. And the last one is the continuous thrust variable specific impulse model, which models electric rocket engines and shall not be explored in this work.

The application of optimal control to the field of orbital maneuvering is mainly concerned with the preservation of propellant. Suppose a satellite has an orbital state $\mathbf{x}_i$ and is required to maneuver to an orbital state $\mathbf{x}_f$ in a time t_f, and it is desired to minimize the amount of propellant used. A convenient way of expressing this is to maximize the final mass of the spacecraft, with constraints:

$$\max_{\mathbf{F}(t)} \quad m(t_f) \tag{2.34}$$

$$\mathbf{x}(0) = \mathbf{x}_i \tag{2.35}$$

$$\mathbf{x}(t_f) = \mathbf{x}_f \tag{2.36}$$

2.3.1   Constant specific impulse model

Chemical and cold gas thrusters are characterized by an exhaust velocity v_e at which the propellant flow is ejected from the spacecraft. With a propellant flow rate $\dot{m}_p$, the thrust $\mathbf{F}$ is given by

$$\|\mathbf{F}\| = v_e \dot{m}_p \tag{2.37}$$

The propellant flow is deducted from the spacecraft's mass; therefore it can be stated

that $\dot{m} = -\dot{m}_p$. Thus, in this model, the spacecraft's mass is a seventh state variable. A new state vector $\mathbf{x}_m = \begin{bmatrix} \mathbf{r}^T & \mathbf{v}^T & m \end{bmatrix}^T$ is defined and subject to the dynamics

$$\begin{bmatrix} \dot{\mathbf{r}} \\ \dot{\mathbf{v}} \\ \dot{m} \end{bmatrix} = \begin{bmatrix} \mathbf{v} \\ -\frac{\mu}{\|\mathbf{r}\|^3}\mathbf{r} + \frac{\mathbf{F}}{m} \\ -\frac{\|\mathbf{F}\|}{v_e} \end{bmatrix} \tag{2.38}$$

In addition, thrusters have limited flow rates, which imposes a maximum thrust magnitude $F_{\max}$:

$$\|\mathbf{F}\| \leq F_{\max} \tag{2.39}$$

The objective from Equation (2.34) can be developed for this model by integrating $\dot{m}$ as

$$m(t_f) = m(0) - \int_0^{t_f} \frac{\|\mathbf{F}\|}{v_e} dt \tag{2.40}$$

Let $\boldsymbol{\Gamma}$ be the acceleration due to thrust such that $\boldsymbol{\Gamma} = \frac{\mathbf{F}}{m}$. The literature (CONWAY, 2010) then suggests considering that the propellant consumption is small compared to the total mass of the satellite, such that it can be stated that

$$m(t_f) \approx m(0) - \frac{m(0)}{v_e} \int_0^{t_f} \|\boldsymbol{\Gamma}\| dt \tag{2.41}$$

Therefore the objective can be restated as

$$\min_{\boldsymbol{\Gamma}(t)} \int_0^{t_f} \|\boldsymbol{\Gamma}\| dt \tag{2.42}$$

subject to $\|\boldsymbol{\Gamma}(t)\| \leq \Gamma_{\max}$ at all times, with $\Gamma_{\max} = \frac{F_{\max}}{m(0)}$.

If the control variable is set to be $\boldsymbol{\Gamma}$ instead of $\mathbf{F}$, this leads to a mass-independent problem. This approximation leads to primer vector theory, and is therefore important.

2.3.2 Impulsive propulsion model

A very simple propulsion model that allows for easier solution of the orbital maneuvering problem supposes that the propulsive forces are much greater and operate much faster than the gravitational force, introducing discontinuities in velocity. This is called *impulsive thrust*. The propulsion model relies on Tsiolkovsky's Equation (CONWAY, 2010),

$$\Delta v = v_e \ln \left(\frac{m_i}{m_f} \right), \tag{2.43}$$

where Δv is the magnitude of an instantaneous change in velocity, v_e is the engine's exhaust velocity (which is treated as a known parameter), m_i is the initial spacecraft mass and m_f is the final mass. Supposing a burn happens at time t_b, the propulsion model can then be expressed through a Dirac delta as

$$\left.\frac{F}{m}\right|_{t=t_b} = \delta(t - t_b)v_e \ln\left(\frac{m(t_b^-)}{m(t_b^+)}\right) = \delta(t - t_b)\Delta v, \tag{2.44}$$

which yields a velocity discontinuity

$$\|\mathbf{v}(t_b^+) - \mathbf{v}(t_b^-)\| = v_e \ln\left(\frac{m(t_b^-)}{m(t_b^+)}\right) = \Delta v. \tag{2.45}$$

Now, between impulses there are coasting arcs where the vessel is subject only to external (gravitational) forces, as illustrated in Figure 2.3. Considering a generic maneuver with n burns, there are $n + 1$ coasting segments related by the change in velocity $\Delta\mathbf{v}_j$ associated with the j-th burn. Considering burn times t_j, with $t_f \geq t_{j+1} \geq t_j \geq 0$, and the initial and final times 0 and t_f, the system is subject to boundary conditions

$$\mathbf{x}(0) = \mathbf{x}_i \tag{2.46}$$

$$\mathbf{r}(t_j^+) = \mathbf{r}(t_j^-), \qquad\qquad \forall j = 1, \ldots, n \tag{2.47}$$

$$\mathbf{v}(t_j^+) = \mathbf{v}(t_j^-) + \Delta\vec{v}_j, \qquad\qquad \forall j = 1, \ldots, n \tag{2.48}$$

$$\mathbf{x}(t_f) = \mathbf{x}_f \tag{2.49}$$

and to dynamical Equation (2.15) in the intermediate times. Using the concept of orbit propagator, this adds the constraints

$$\mathbf{x}(t_1^-) = p_o(\mathbf{x}(0), t_1) \tag{2.50}$$

$$\mathbf{x}(t_{j+1}^-) = p_o(\mathbf{x}(t_j^+), t_{j+1} - t_j), \forall j = 1, \ldots, n - 1 \tag{2.51}$$

$$\mathbf{x}(t_f) = p_o(\mathbf{x}(t_n^+), t_f - t_n) \tag{2.52}$$

to the previous list. Each impulse is described by its time t_j and its velocity change vector $\Delta\mathbf{v}_j$. Accounting for $\mathbf{x}(0)$, all of the intermediate $\mathbf{r}(t_j^-)$, $\mathbf{r}(t_j^+)$, $\mathbf{v}(t_j^-)$ and $\mathbf{v}(t_j^+)$, and also the final state $\mathbf{x}(t_f)$, plus the impulse parameters, there are $6 + 12n + 6 + 4n = 16n + 12$ unknowns. At the same time, there are $6 + (3 + 3)n + 6 + 6 + 6(n - 1) + 6 = 12n + 18$ constraints. Therefore, for general initial and final conditions, the *minimal number of impulses* is 2.

Tsiolkovsky's equation can be applied to all impulses, thus relating the final and initial masses with the total velocity change, which is the sum of all n burns executed during
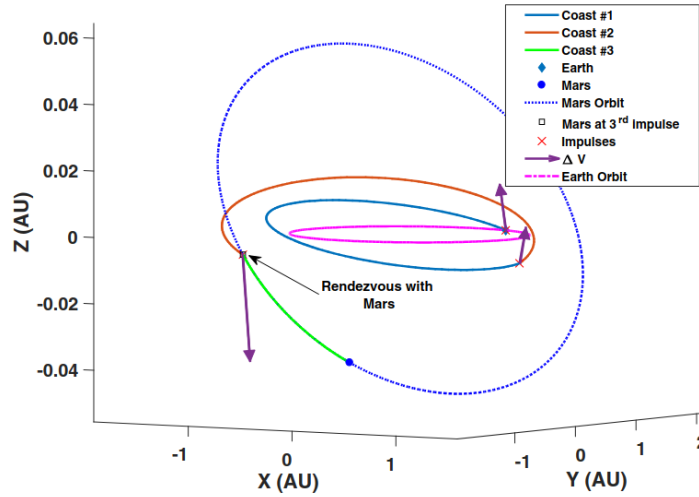
FIGURE 2.3 – illustration of impulsive transfer with Eart to Mars transfer in 3 impulses. Source: (TAHERI; JUNKINS, 2019).

the transfer:

$$m(t_f) = m(0) \exp \left(-\frac{\sum_{i=1}^{n} \Delta v_i}{v_e} \right) \qquad (2.53)$$

Since v_e and $m(0)$ are not subject to optimization, the objective (2.34) is equivalent to minimizing the sum of magnitudes of impulses used during the transfer:

$$\min \sum_{i=1}^{n} \Delta v_i. \qquad (2.54)$$

Thus, in the impulsive case, the problem is *independent of spacecraft mass*, and it can be eliminated from the state vector. However, the control trajectory $\mathbf{\Gamma}(t)$ in the impulsive case is not a function, but a *measure*. It therefore needs to be implemented not as a function of time, as usual in optimal control, but as magnitudes of discontinuities in the state trajectory. This introduces the number of allowed impulses as an optimization hyperparameter (LEANDER *et al.*, 2015). To choose an optimal number of impulses, the theory of primer vectors (see ahead) can help determine the number of impulses needed (LUO *et al.*, 2010).

2.3.2.1   Hohmann transfer

The prototypical orbital maneuver case is that of a two-impulse transfer between two coplanar circular orbits in Keplerian dynamics (CHOBOTOV, 2002). The intermediate orbit, between the two impulses, is an ellipse that is tangent to both initial and final orbits, as can be seen in Figure 2.4. This transfer has a known analytical optimal, which can be proven by several different methods. Some useful quantities relating to this transfer
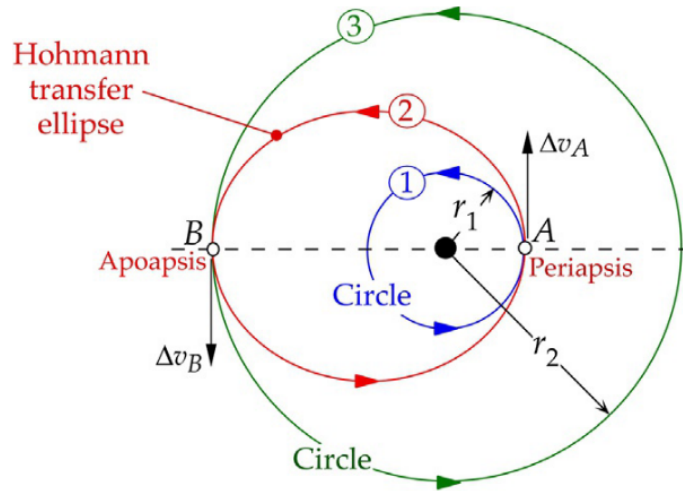
FIGURE 2.4 – Hohmann transfer diagram. Source: (CURTIS, 2020)

are given in the following. Given an initial circular orbit of semi-major axis a_1 and a final circular orbit with semi-major axis a_2, the total change in speed required is equal to (CHOBOTOV, 2002):

$$\sum \|\Delta \mathbf{v}\| = \sqrt{\mu \left(\frac{2}{a_1} - \frac{2}{a_1 + a_2} \right)} - \sqrt{\frac{\mu}{a_1}} + \sqrt{\frac{\mu}{a_2}} - \sqrt{\mu \left(\frac{2}{a_2} - \frac{2}{a_1 + a_2} \right)} \qquad (2.55)$$

The transfer time is half of the transfer orbit's period. With t_H being the Hohmann transfer duration, is is given by (CHOBOTOV, 2002)

$$t_H = \pi \sqrt{\frac{\left(\frac{a_1 + a_2}{2} \right)^3}{\mu}}. \qquad (2.56)$$

2.4 Primer vector theory

The application of optimal control theory to orbital maneuvers dates back to the 1960s, with pioneering work by Lawden (CONWAY, 2010). In particular, he coined the term "primer vector" as an analogy with the fact that the costate trajectory imposes a necessary condition for firing the engines, thus acting as a "primer". This theory is based on the indirect necessary conditions provided by the Hamiltonian formalism previously exposed, and is explored in Conway (2010). Here, the impulsive thrust case will be treated as a limiting case of finite thrust when $\Gamma_{\max} \to \infty$.

2.4.1 Conservative Orbital model

Firstly, a model where $\ddot{\mathbf{r}} = g(\mathbf{r}) = \nabla\Phi(\mathbf{r})$, where $\Phi(\mathbf{r})$ is a gravitational potential field, is considered. This type of model contains the two body approach as well as the J2 model.

The acceleration due to the thrust $\boldsymbol{\Gamma}$ can be split into its magnitude and direction as $\boldsymbol{\Gamma} = \Gamma\hat{\mathbf{u}}$, $\Gamma = \|\boldsymbol{\Gamma}\|$, $\|\hat{\mathbf{u}}\| = 1$ so that the objective from Equation (2.42) can be rewritten as

$$\min_{\Gamma(t),\hat{\mathbf{u}}(t)} \int_0^{t_f} \Gamma dt \tag{2.57}$$

and the Hamiltonian of the system is the given by

$$H = \Gamma + \begin{bmatrix} \lambda_r^T & \lambda_v^T \end{bmatrix} \begin{bmatrix} \mathbf{v} \\ g(\mathbf{r}) + \Gamma\hat{\mathbf{u}} \end{bmatrix} \tag{2.58}$$

The costate is subject to the adjoint equations given in block matrix form as

$$\begin{bmatrix} \dot{\lambda}_r \\ \dot{\lambda}_v \end{bmatrix} = \begin{bmatrix} 0_{3\times3} & -\left(\frac{\partial g(\mathbf{r})}{\partial \mathbf{r}}\right)^T \\ -I_{3\times3} & 0 \end{bmatrix} \begin{bmatrix} \lambda_r \\ \lambda_v \end{bmatrix} \tag{2.59}$$

which is linear in the costate variables. For problems with final position and velocity constraints, no boundary conditions are given for the adjoint equations.

Rearranging the Hamiltonian to factor Γ,

$$H = (1 + \lambda_v^T\hat{\mathbf{u}})\Gamma + \lambda_r^T\mathbf{v} + \lambda_v^T g(\mathbf{r}). \tag{2.60}$$

By applying Pontryagin's Minimum Principle, the thrust magnitude Γ is given piecewise by analyzing the sign of its coefficient:

$$\Gamma = \begin{cases} \Gamma_{\max} & , 1 + \lambda_v^T\hat{\mathbf{u}} < 0 \\ 0 & , 1 + \lambda_v^T\hat{\mathbf{u}} > 0 \\ \text{intermediate} & , \text{otherwise} \end{cases} \tag{2.61}$$

The case where $1 + \lambda_v^T\hat{\mathbf{u}} = 0$ on a finite interval of time will not be considered here; these are *singular arcs* and occur rarely (MORELLI *et al.*, 2023). When $\Gamma = \Gamma_{\max}$, its coefficient should be as negative as possible, which happens when $\hat{\mathbf{u}}$ has the opposite direction to λ_v:

$$\hat{\mathbf{u}} = -\frac{\lambda_v}{\|\lambda_v\|}. \tag{2.62}$$

This direction, the *optimal thrust direction* given by $-\lambda_v$ is what constitutes the primer

vector $\mathbf{p}$, which is defined as

$$\mathbf{p} = -\lambda_v. \tag{2.63}$$

The engine firing conditions can be stated solely as a function of the primer vector as (CONWAY, 2010)

$$\Gamma = \begin{cases} \Gamma_{\max} & , \|\mathbf{p}\| > 1 \\ 0 & , \|\mathbf{p}\| < 1 \\ \text{intermediate} & , \text{otherwise} \end{cases} \tag{2.64}$$

The impulsive thrust case is then found by letting $\Gamma_{\max} \to \infty$, in which case the segments where $\|\mathbf{p}\| > 1$ approach points, and the thrust cases become

$$\Gamma = \begin{cases} 0 & , \|\mathbf{p}\| < 1 \\ \Delta\mathbf{v}\delta & , \|\mathbf{p}\| = 1 \end{cases}, \tag{2.65}$$

for some (possibly null) velocity increment $\Delta\mathbf{v}$

Alternatively, one could reason about the constant value of the Hamiltonian which, from Equation (2.13), is finite. Therefore, at the impulse instants, where Γ is unbounded, its coefficient $1 + \lambda_v^T \hat{\mathbf{u}}$ must be 0, leading to $\hat{\mathbf{u}} = -\lambda_v = \mathbf{p}$, and the condition $\|\mathbf{p}\| = 1$.

The necessary conditions offered by primer vector theory for an impulsive maneuver scenario are (CONWAY, 2010):

1. $\mathbf{p}(t)$ and $\dot{\mathbf{p}}(t)$ are continuous;

2. $\|\mathbf{p}\| \leq 1$;

3. $\mathbf{p} = \hat{\mathbf{u}}$ at the impulse instants, with the corollary that when an impulse happens, $\|\mathbf{p}\| = 1$;

4. $\frac{d\|\mathbf{p}\|}{dt} = 0$ at impulses between the initial and final times (non-inclusive).

In addition to these conditions for the optimal solution, variational calculus results can give some insight into how to change a suboptimal trajectory based on how those conditions are violated (CONWAY, 2010). For a maneuver with start time between times 0 and t_f, these results can be enumerated:

1. If the maneuver starts with an impulse ($\|\mathbf{p}(0)\| = 1$) and $\partial_t \|\mathbf{p}\| \mid_{t=0} > 0$, adding an initial coast will lower the cost;

2. If the maneuver ends with an impulse ($\|\mathbf{p}(t_f)\| = 1$) and $\partial_t \|\mathbf{p}\| \mid_{t=0} < 0$, adding a final coast will lower the cost;

3. If $\|\mathbf{p}(t)\| > 1$ for some $t \in [0, t_f]$, adding an impulse will lower the cost.

2.4.1.1 Primer vector calculation

From Equations (2.59) and (2.63), the primer vector differential equations are

$$\begin{bmatrix} \dot{\mathbf{p}} \\ \ddot{\mathbf{p}} \end{bmatrix} = \begin{bmatrix} \mathbf{0}_3 & \mathbf{I}_3 \\ \left[\frac{\partial g}{\partial \mathbf{r}}\right]^T & \mathbf{0}_3 \end{bmatrix} \begin{bmatrix} \mathbf{p} \\ \dot{\mathbf{p}} \end{bmatrix} = \mathbf{A}_p \begin{bmatrix} \mathbf{p} \\ \dot{\mathbf{p}} \end{bmatrix} \tag{2.66}$$

Since Equation (2.66) is linear on the variables, it admits a solution through the form of a primer vector transition matrix (PVTM) $\mathbf{\Phi}_p(t - t_0)$ such that

$$\begin{bmatrix} \mathbf{p}(t) \\ \dot{\mathbf{p}}(t) \end{bmatrix} = \mathbf{\Phi}_p(t - t_0) \begin{bmatrix} \mathbf{p}(t_0) \\ \dot{\mathbf{p}}(t_0) \end{bmatrix}. \tag{2.67}$$

However, since $g = \nabla\Phi = \left(\frac{\partial \Phi}{\partial \mathbf{r}}\right)^T$, $\left[\frac{\partial g}{\partial \mathbf{r}}\right]$ is actually the Hessian matrix of the potential field, which is symmetric. Therefore, the primer vector is subject to the same differential equation as the STM in Equation (2.30), and Equation (2.32) can be used to equate the PVTM to the STM:

$$\mathbf{\Phi}_p(t - t_0) = \mathbf{\Phi}_\delta(t - t_0) = \frac{\partial \mathbf{x}(t)}{\partial \mathbf{x}(t_0)}. \tag{2.68}$$

This way of computing $\mathbf{\Phi}_p(t - t_0)$ will be termed the STM method for primer vector calculation, and is valid for all conservative force models. For the two body model in particular, a closed form for $\mathbf{\Phi}_p(t - t_0)$ exists (GLANDORF, 1969).

Computing the primer vector trajectory is done piecewise on coasting arcs between two consecutive impulses, since the primer vector is known at impulse times. Since $\mathbf{p}$ is known at both ends, but not $\dot{\mathbf{p}}$, this configures a linear TPBVP. For two consecutive impulses, Δv_1 at time t_1 and Δv_2 at time t_2, the primer vector values are given by:

$$\mathbf{p}(t_1) = \frac{\Delta \mathbf{v}_1}{\|\Delta \mathbf{v}_1\|} \tag{2.69}$$

$$\mathbf{p}(t_2) = \frac{\Delta \mathbf{v}_1}{\|\Delta \mathbf{v}_2\|} \tag{2.70}$$

The state transition between these two instants can be stated as

$$\begin{bmatrix} \mathbf{p}(t_2) \\ \dot{\mathbf{p}}(t_2) \end{bmatrix} = \mathbf{\Phi}_p(t_2 - t_1) \begin{bmatrix} \mathbf{p}(t_1) \\ \dot{\mathbf{p}}(t_1) \end{bmatrix} = \begin{bmatrix} \mathbf{M}(t_2 - t_1) & \mathbf{N}(t_2 - t_1) \\ \mathbf{S}(t_2 - t_1) & \mathbf{T}(t_2 - t_1) \end{bmatrix} \begin{bmatrix} \mathbf{p}(t_1) \\ \dot{\mathbf{p}}(t_1) \end{bmatrix} \tag{2.71}$$

where $\mathbf{M}$, $\mathbf{N}$, $\mathbf{S}$ and $\mathbf{T}$ are square matrices. From now on the times shall be denoted as indices for conciseness. If $\mathbf{p}$ and $\dot{\mathbf{p}}$ are known for a certain time, the entire trajectory can

be found. It is easy to isolate $\dot{\mathbf{p}}_1 = \dot{\mathbf{p}}(t_1)$:

$$\dot{\mathbf{p}}_1 = \mathbf{N}_{21}^{-1} \left(\mathbf{p}_2 - \mathbf{M}_{21} \mathbf{p}_1 \right). \tag{2.72}$$

$\mathbf{N}_{21}$ is invertible except for isolated values of t (CONWAY, 2010); in these cases, the primer vector trajectory is assumed to lie in the orbital plane, spanned by $\begin{bmatrix} \mathbf{r}_1 & \mathbf{v}_1 \end{bmatrix}$. Thus, for singular N,

$$\dot{\mathbf{p}}_1 = \begin{bmatrix} \mathbf{r}_1 & \mathbf{v}_1 \end{bmatrix} \left(\mathbf{N}_{21} \begin{bmatrix} \mathbf{r}_1 & \mathbf{v}_1 \end{bmatrix} \right)^{\dagger} \left(\mathbf{p}_2 - \mathbf{M}_{21} \mathbf{p}_1 \right) \tag{2.73}$$

where $A^{\dagger}$ denotes the pseudo-inverse of a rectangular matrix.

2.4.2 Non-conservative Orbital model

Here, the model considered has a conservative part $g(\mathbf{r})$ and a non-conservative part $d(\mathbf{r}, \mathbf{v})$, representing drag, or other non-conservative forces, such that $\ddot{\mathbf{r}} = g(\mathbf{r}) + d(\mathbf{r}, \mathbf{v})$.

The Hamiltonian of the system is the given by

$$H = \Gamma + \begin{bmatrix} \lambda_r^T & \lambda_v^T \end{bmatrix} \begin{bmatrix} \mathbf{v} \\ g(\mathbf{r}) + d(\mathbf{r}, \mathbf{v}) + \Gamma \hat{\mathbf{u}} \end{bmatrix} \tag{2.74}$$

The costate is subject to the adjoint equations given in block matrix form as

$$\begin{bmatrix} \dot{\lambda}_r \\ \dot{\lambda}_v \end{bmatrix} = \begin{bmatrix} 0_{3 \times 3} & -\left[\frac{\partial}{\partial \mathbf{r}} \left(g(\mathbf{r}) + d(\mathbf{r}, \mathbf{v}) \right) \right]^T \\ -I_{3 \times 3} & -\left(\frac{\partial d(\mathbf{r}, \mathbf{v})}{\partial \mathbf{v}} \right)^T \end{bmatrix} \begin{bmatrix} \lambda_r \\ \lambda_v \end{bmatrix}. \tag{2.75}$$

Rearranging the Hamiltonian to factor Γ,

$$H = (1 + \lambda_v^T \hat{\mathbf{u}}) \Gamma + \lambda_r^T \mathbf{v} + \lambda_v^T (g(\mathbf{r}) + d(\mathbf{r}, \mathbf{v})). \tag{2.76}$$

By similar reasoning to the conservative case, $\mathbf{p} = -\lambda_v$, with the same necessary conditions.

2.4.2.1 Primer Vector calculation

The primer vector differential equation is the main difference of the non-conservative case w.r.t. the conservative case. It can be found from Equation (2.75):

$$\begin{bmatrix} \dot{\mathbf{p}} \\ \ddot{\mathbf{p}} \end{bmatrix} = \begin{bmatrix} \mathbf{0}_3 & \mathbf{I}_3 \\ \left[\frac{\partial}{\partial \mathbf{r}} \left(g(\mathbf{r}) + d(\mathbf{r}, \mathbf{v}) \right) \right]^T & -\left(\frac{\partial d(\mathbf{r}, \mathbf{v})}{\partial \mathbf{v}} \right)^T \end{bmatrix} \begin{bmatrix} \mathbf{p} \\ \dot{\mathbf{p}} \end{bmatrix} = \mathbf{A}_p \begin{bmatrix} \mathbf{p} \\ \dot{\mathbf{p}} \end{bmatrix}. \tag{2.77}$$

Save some very particular non-conservative force models, the non-conservative primer vector dynamics in Equation (2.77) is **not** equal to the non-conservative variational perturbation differential equation, which disallows the STM method from being used. However, it remains a linear differential equation with transition matrix $\mathbf{\Phi}_p(t - t_0)$ subject to

$$
\begin{cases}
\dot{\mathbf{\Phi}}_p = \mathbf{A}_p(\mathbf{r}, \mathbf{v})\mathbf{\Phi}_p \\
\mathbf{\Phi}_p(0) = \mathbf{0}_6
\end{cases}
, \tag{2.78}
$$

which allows for the solution of a linear TPBVP as described in Equations (2.69)-(2.73).

2.4.3 Primer vector theory summary

method of calculation x model

necessary conditions

3 Bibliographic review

In this chapter, previous results relating to the field of orbital maneuvering are presented. Relevant research spans the 1960's all the way to recent years. In particular, results about the solution and application of the Lambert problem, usage of primer vector theory and direct optimization approaches are presented.

TODO add Multiple shooting

TODO cite numerical integration

3.1 Primer Vector theory

The evolution of the primer vector along coasting arcs is of interest for the solution of impulsive maneuvering problems. An analytical form of the state transition matrix is given in GLANDORF (1969). A clever choice of time-changing basis allows for the direct solution of the components of the primer vector differential equations (Lagrange multiplier equations), which can then be written in matrix form. The state transition matrix is given as the product of a time-evolving matrix with its inverse at the initial time; closed form expressions are given for the 6×6 state transition matrix. Despite being restricted to the two body problem, this result proves really useful since it allows the circumvention of the solution of a TPBVP.

LION; HANDELSMAN (1968) also give a closed-form expression for the state transition matrix and a review of the application of primer vector theory. In particular, several common cases of primer vector trajectories are explored, and the relationship between suboptimal primer vector trajectories and the necessary changes is explored. Overall, Lion and Handelsman provide useful examples for understanding this theory.

Finally, an interactive algorithm for computing the optimal number of impulses based on analyzing the primer vector trajectories is given in LUO *et al.* (2010). The discrete nature of the variable "number of impulses" requires tools more powerful than continuous variable nonlinear solvers, such as evolutionary algorithms. The proposed algorithm iterates through proposing an n impulse maneuver, analyzing its primer vector history and

optimizing impulse times, if needed, and then adding maneuvers if the necessary conditions are not yet satisfied. This remains one of the most direct ways of optimizing the number of impulses; however, the usage of primer vector theory provides only *necessary* conditions, which can lead to many false (or local) optima. Similar approaches are found in JEZEWSKI; ROZENDAAL (1968), which applies it to an Apollo rendezvous, with a large plane change maneuver.

TODO ADD RYAN RUSSELL, BRUNO

3.2   Direct Optimization

The central question of how many impulses are needed for a maneuver is tackled through the continuous-thrust approach in TAHERI; JUNKINS (2019). A continuous thrust model is established and a sequence of increasing maximum thrust values is analyzed. Starting with the minimum thrust needed to execute the maneuver in the given time (case in which the engines fire incessantly), the thrust is continuously increased, and gaps in the thrusting times appear. In the limiting case of very high thrusts approaching infinity, engine firing closely resembles an impulse. This gives, to very good approximation, the needed number of impulses. The main disadvantage of this approach is the need for a continuous thrust model, in addition to an impulse thrust model.

A similar approach is presented in ARYA *et al.* (2023), where a "control sweep" is performed to identify how many impulses are necessary, thus excluding the number of impulses as a problem variable. In particular, both continuous thrust constant specific impulse problems and continuous thrust variable specific impulse problems (not treated in the present work) are used during this step. These problems help in finding better optima in multi-revolution maneuvers, where multiple local optima exist. In addition, the importance of impulsive solutions is reaffirmed. Despite being abstractions, impulsive solutions provide lower bounds on fuel usages, can provide feasibility insights and can be abstracted from spacecraft mass.

The existence of multiple global optima is explored in SALOGLU *et al.* (2023), which proposes a method for generating families of transfer orbits with many impulses starting with a seed two-impulse maneuver. From a theoretical point of view, this highlights the non-convexity of the orbital maneuver optimization problem (existence of many optima), often tied to the periodicity of orbits. From a practical point of view, it exposes the concept of *phasing orbit*, an intermediate orbit between two consecutive impulses that can be chosen arbitrarily from certain period values without changing the delta-V budget. Also, the possibility of reducing flight time based on some of those solutions is also explored. However, these results are mostly applicable to long time horizon problems.

In PRUSSING; CHIU (1986), multiple impulse maneuvers for fixed time rendez-vous between spacecraft in a subclass of circular orbits is considered. The fixed time rendez-vous problem is analogous to the problem of transfer to a particular state in fixed time. Despite the restriction to a subset of possible orbits, it is shown that there is a certain minimum time required for the optimal time-open solutions (such as Hohmann transfers) to be found. Again, primer vector theory is applied but sometimes leads to local optima, and divergences from the established primer vector algorithm can sometimes be preferred over following it stricly.

4 Methodology

All code was implemented in the Julia language due to the availability of *packages* for subproblems of this work. In the next section, several components of the solution to the problem of optimization of impulsive maneuvers are detailed, and the following section assembles all components into the full optimization algorithm.

TODO orbital models used

TODO STM methods

4.1 Components

The optimization of impulsive maneuvers relies on the representation and manipulation of several concepts in a programmatic fashion. In particular there is a need for a nonlinear numerical solver, a numerical way of propagating orbits, a representation for sequences of impulses and coasting arcs, an implicit formulation for maneuvers amenable to optimization, and a way of calculating primer vector trajectories on multi-impulse maneuvers. Each of those components will be explored in the following sections.

4.1.0.1 Nonlinear solver

Nonlinear solvers are algorithms which iteratively approximate the solution to a system of nonlinear equations or a constrained optimization problem. Their choice is problem dependent and problems must be stated in a format compatible with the desired solver. Many algorithms exist, with different smoothness requirements, convergence properties, or optimality guarantees.

Of interest to this work are local gradient-based algorithms. They are well suited to nonlinear (but twice differentiable) problems with continuous variables subject to nonlinear constraints. By exploiting the gradient, and sometimes the Hessian of the cost as well, faster algorithms are available. The downside of this type of algorithm is that they return a *local* solution, that is, a solution where no small change can improve it.

Those are, in general, not *global* solutions. Orbital maneuver problems have many local solutions of varying qualities, meaning that this distinction must be accounted for. The algorithm takes an initial guess as a parameter and improves it, simultaneously satisfying constraints and minimizing the objective function.

Julia offers a multitude of nonlinear solvers, each with different scope, interface, and algorithms. This work has chosen to use `CasADi` (ANDERSSON *et al.*, 2019), a package which offers a modelling language for optimization problems that is quite close to mathematical notation, and is the industry standard for optimal control. Internally, CasADi converts the problem to a format accepted by Ipopt (WäCHTER; BIEGLER, 2006), the default nonlinear solver in CasaDi. Ipopt is an open-source nonlinear solver widely recognized for its speed and precision, outperforming many competitors and being quite flexible. It is especially well suited to problems with many variables (up to thousands) with sparse constraints (that is, constraints that depend only on small subsets of variables). It is a Newton-like algorithm with many optimizations to iteration acceptance criteria, filtering of bad iterates, and many configurable parameters. Internally, this means that Ipopt must solve very large linear systems (Jacobian inversion) as a part of the solve process, which introduces normalization concerns (discussed later).

This solver allows for the specification of lower and upper bounds of variables separately to the specification of inequality constraints. Variable bounds are guaranteed to be respected at all iterations; inequality constraints are only guaranteed to be satisfied at the converged solution, if the problem is feasible. This distinction is important because some constraints define the domain of problem and should never be violated, such as positivity of time durations; other constraints are problem-based and therefore can be violated during the iteration process.

Ipopt uses a barrier function method to handle constraints. This means that the initial guess is not *required* to satisfy all constraints and, in all iterations except the final, converged iterate, constraint violation is allowed. The user-input cost function is replaced by a mixed objective containing the cost function a cost on constraint violation. During iteration, constraint violation is increasingly penalized until a solution in the feasible set is found, where optimization can continue. A corollary of this scheme is that even if the initial guess is very close to satisfying some constraints, but not others, intermediate iterates may worsen constraint violation and objective function in favor of this mixed objective.

Ipopt also comes with a host of configuration options. Parameters worth mentioning are the tolerance for constraint violation, maximum iteration count, maximum solve time, and maximum *restoration iterations*. Restoration iterations are iterations in which no attempt to improve the objective function is made, and the solver focuses only on satisfying constraints. This usually happens when constraints are "hard", the feasible region of the

problem is small, or iterates diverge. Limiting this reduces time wasted on trying to optimize a bad initial guess.

4.1.1 Orbit Propagation

The implementation of an orbit propagator concerns itself with the implementation of the function $p_o(\mathbf{x}, t)$ introduced in Equation (2.21). Two different cases are to be considered: "explicit" propagation, where numerical inputs are available and a numerical output is desired; and "implicit" propagation, where the propagation step is a part of a larger solver.

Brazil's National Institute of Space Research (INPE) developed a package for orbit propagation and analysis with several models (Kepler, J2 semi-analytical secular and short term, among others) called `SatelliteToolbox` (CHAGAS *et al.*, 2025). It provides quite convient functions for converting between the Cartesian state vector $\begin{bmatrix} \mathbf{r}^T & \mathbf{v}^T \end{bmatrix}^T$ and the Keplerian elements, as well as functions for the propagation of orbits by some specified amount of time t_p. Its algorithms were chosen with precision around edge cases in mind (SCHWARZ, 2014), making it numerically precise but unsuitable for nonlinear solvers, which expect differentiable functions everywhere. The functions in this package are also limited to elliptic orbits, which are not guaranteed to be found during iteration inside a numerical solver like Ipopt.

Therefore, this is an auxiliary package used for verification, initial guess generation, and direct numerical propagation whenever required. When propagation is required in the statement of a nonlinear optimization problem, another method for orbit propagation is required. Despite being useful for explicit propagation, Keplerian elements are unsuited for optimization (at least with the chosen solver, see Section 4.1.0.1). This can be seen from the equation relating the true anomaly θ and the eccentric anomaly E, Equation (2.20), discussed in Table 4.1. In summary, the anomaly equations require special treatment close to the apogee to avoid infinities or discontinuities.

Form	LHS value at apogee	RHS value at apogee	Comment
$\tan \frac{\theta}{2} = \sqrt{\frac{1+e}{1-e}} \tan \frac{E}{2}$	$+\infty$	$+\infty$	Value unsuitable for computation
$\theta = 2\arctan \sqrt{\frac{1+e}{1-e}} \tan \frac{E}{2}$	π	$\pm\pi$	Not continuous $\therefore$ not differentiable

TABLE 4.1 – Problems with the Keplerian elements formulation exemplified with the relationship between eccentric and true anomalies

Therefore, the dynamics in Cartesian coordinates were chosen for implicit propagation,

due to the differentiability of this model in the usual range of orbital variables. Many methods for integrating dynamical systems for optimal control exist, such as collocation, pseudospectral methods, direct shooting, and multiple shooting (PRESS *et al.*, 2007). Multiple shooting was chosen since it leads to a numerically stable problem and is standard in optimal control. An eighth-order Runge-Kutta (RK8) method (VERNER, 2010) was used for discretizing the dynamical equations. Let $\mathbf{x}_{\text{next}} = f_{RK}(\mathbf{x}_{\text{prev}}, \Delta t)$ be the RK8 integration function from Cartesian state $\mathbf{x}_{\text{prev}}$ to Cartesian state $\mathbf{x}_{\text{next}}$ over a time step Δt. This discretization scheme is agnostic to the dynamics of the system, that is, one can "drop-in" the two body model, the J2 model, or the J2-Drag model and the scheme remains the same, which is quite convenient.

The multiple shooting implicit orbit propagation uses N discretization points for a coasting arc of duration d_c, which are parameterized with Cartesian state vector variables $\mathbf{x}^j \in \mathbb{R}^6, j = 1, \ldots, N$ subject to

$$\mathbf{x}^{j+1} = f_{RK}(\frac{d_c}{N-1}, \mathbf{x}^j), j = 1, \ldots, N. \tag{4.1}$$

To complete the implicit description, $\dim \mathbf{x} = 6$ boundary conditions are needed. These may be an initial condition, a final condition, or an impulsive boundary condition between two arcs.

4.1.2 Maneuver Propagation

Impulsive maneuvers are characterized by a sequence of impulses and coasting arcs. A notation for maneuvers is introduced, where `C` represents a coasting arc, and `I` represents an impulse. Any alternating sequence $\mathcal{S} \in \{$`C`, `I`$\}^{n_c + n_i}$, where n_c is the number of coasting arcs and n_i is the number of impulses, with 2 or more impulses makes a valid maneuver: `ICI`, `ICIC`, `CICICICIC`, etc. Maneuvers need at least 2 impulses to be able to take any initial state to any final state (see Section 2.3.2). Also, let $\mathcal{I} = \{i \in 1, \ldots, n_i + n_c | \mathcal{S}_i = $ `I`$\}$ and $\mathcal{C} = \{c \in 1, \ldots, n_i + n_c | \mathcal{S}_c = $ `C`$\}$ be the sets of impulse and coast indices respectively. Figure 4.1 illustrates the algorithm for propagating a maneuver: at impulses, a velocity discontinuity is applied; at coasting arcs, the orbit is propagated. This algorithm follows the specified sequence of maneuvers for given values of impulse magnitudes and directions, and coast durations.

Implicit maneuver propagation is required for optimization. For this, coasts are parameterized according to the multiple shooting scheme of last section, and impulsive boundary conditions between arcs are added as constraints.
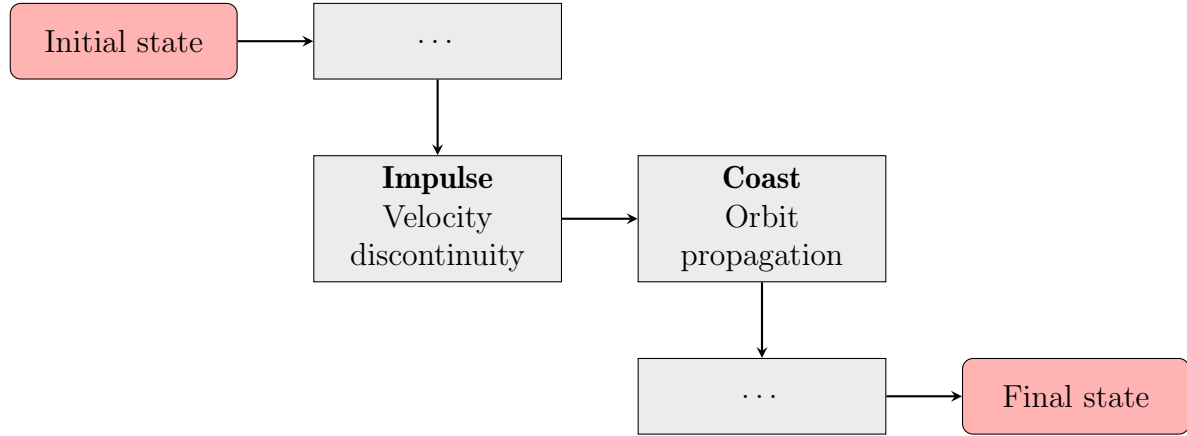
FIGURE 4.1 – Maneuver propagation scheme.

4.1.3 Maneuver multiple shooting problem statement

The full maneuver optimization problem, in its multiple shooting formulation, shall be stated in this section. The input parameters are:

1. $\mathbf{r}_1$, $\mathbf{v}_1$: initial orbital position and velocity;

2. $\mathbf{r}_2$, $\mathbf{v}_2$: final orbital position and velocity;

3. t_f: transfer time;

4. N: number of integration steps per coasting arc.

5. $\mathcal{S} \in \{\mathtt{C}, \mathtt{I}\}^{n_c + n_i}$: the desired sequence of coasts and impulses.

The problem's definition and variable set dynamically depends on the input sequence. The i-th impulse is described by the variables[1]

1. $\Delta v_i \geq 0$: magnitude of the impulse;

2. $\hat{\mathbf{u}}_i \in \mathbb{R}^3$: direction of the impulse.

The c-th coasting arc is described by:

1. $d_c \geq 0$: total duration of the arc;

2. $\mathbf{x}_c^j \in \mathbb{R}^6, j = 1, \ldots, N$: tate vector variables for each coasting arc.

---

[1]The problem could have been parameterized with vector quantities for the changes in velocities, $\Delta \vec{\mathbf{v}}$, but the objective function would then be stated $\sum \sqrt{\Delta \vec{\mathbf{v}}^T \Delta \vec{\mathbf{v}}}$, which is not differentiable at $\Delta \vec{\mathbf{v}} = 0$, which is inconvenient.

Some care needs to be taken about the first sequence element, an impulse or coast, since this changes the necessary constraints for the initial and final conditions. The full multiple shooting problem for the optimization of the impulsive maneuver is:

$$
\begin{aligned}
\min_{\substack{\Delta v_i \in \mathbb{R}_+, i \in \mathcal{I}, \\ \hat{\mathbf{u}}_i \in \mathbb{R}^3, i \in \mathcal{I}, \\ d_c \in \mathbb{R}_+, c \in \mathcal{C}, \\ \mathbf{x}_c^j \in \mathbb{R}^6, j = 1, \ldots, N, c \in \mathcal{C}}} \quad & \sum_{i \in \mathcal{I}} \Delta v_i
\end{aligned}
$$

subject to:

Total time	$\sum_{c \in \mathcal{C}} d_c = t_f$
Unit directions	$\hat{\mathbf{u}}_i^T \hat{\mathbf{u}}_i = 1, i \in \mathcal{I}$
Propagation of coasts	$\mathbf{x}_c^{j+1} = f_{RK}(\frac{d_c}{N-1}, \mathbf{x}_c^j),$
	$j = 1, \ldots, N-1, c \in \mathcal{C}$

$$
\begin{aligned}
\text{Impulse boundary conditions} \quad & \mathbf{x}_{i+1}^1 = \mathbf{x}_{i-1}^N + \begin{bmatrix} 0_{3\times 1} \\ \Delta v_i \hat{\mathbf{u}}_i \end{bmatrix}, \\
& i \in \mathcal{I}, i \neq 1, n_i + n_c
\end{aligned}
\tag{4.2}
$$

$$
\begin{aligned}
\text{Initial condition} \quad & \mathbf{x}_1^1 = \begin{bmatrix} \mathbf{r}_1 \\ \mathbf{v}_1 \end{bmatrix}, 1 \in \mathcal{C} \\[2mm]
& \mathbf{x}_2^1 = \begin{bmatrix} \mathbf{r}_1 \\ \mathbf{v}_1 + \Delta v_1 \hat{\mathbf{u}}_1 \end{bmatrix}, 1 \in \mathcal{I} \\[2mm]
\text{Final condition} \quad & x_c^N = \begin{bmatrix} \mathbf{r}_2 \\ \mathbf{v}_2 \end{bmatrix}, c = n_i + n_c \in \mathcal{C} \\[2mm]
& x_{i-1}^N + \begin{bmatrix} 0_{3\times 1} \\ \Delta v_i \hat{\mathbf{u}}_i \end{bmatrix} = \begin{bmatrix} \mathbf{r}_2 \\ \mathbf{v}_2 \end{bmatrix}, i = n_i + n_c \in \mathcal{I}
\end{aligned}
$$

As discussed in Section 4.1.0.1, the solver should be initialized with an initial guess that is not far from being feasible. For multiple shooting schemes, this means satisfying the dynamical constraints, but possibly not the final condition constraint. Therefore, initial guesses can be generated by guessing impulse magnitudes and directions, coast durations and applying the maneuver propagation algorithm from Section 4.1.2. Early experimentation shows that coast durations have the biggest impact on the optimization result, so impulse magnitudes can be set to 0. Therefore, to best explore the available solutions and somewhat counteract the local nature of Ipopt, a random sampling scheme was setup, which samples coast durations adding up to the total time and creates a "zero" maneuver composed of coasting arcs along the initial orbit and zero magnitude impulses at specified times. This, combined with early stopping in divergent cases (`max_resto_-iter` mentioned in 4.1.0.1), allowed for speedy optimization of short and mid duration

maneuvers.

Finally, some practical considerations about the multiple shooting scheme are presented.

4.1.3.1 Variable normalization

Cartesian orbital variables regularly take on values on the order of 10^6. At this range of values, floating-point number are more spaced out than on the order of 1, meaning that the optimal values for a problem may lie between two consecutive floating point number representations. In addition, Jacobians evaluated at big variable values tend to be ill-conditioned, leading to worse iterates due to lost precision. All of this leads to the need of normalizing variables.

Variable normalization was done by rescaling physical units for length and time before assembling the multiple shooting problem. Let L be a normalizing length, and T be a normalizing time. Then, a change of units is performed and new, rescaled physical parameters are found. Let $\tilde{\bullet}$ represent the rescaled version of any variable $\bullet$. This procedure is exemplified with the two-body model, but is analogous for the other models explored in the work:

$$\ddot{\mathbf{r}} = -\frac{\mu}{r^3}\mathbf{r} \iff \frac{L}{T^2}\frac{d^2\tilde{\mathbf{r}}}{d\tilde{t}} = -\frac{\mu}{L^2\tilde{r}^3}\tilde{\mathbf{r}} \iff \frac{d^2\tilde{\mathbf{r}}}{d\tilde{t}} = -\frac{\tilde{\mu}}{\tilde{r}^3}\tilde{\mathbf{r}} \tag{4.3}$$

with $\tilde{\mu} = \mu\frac{T^2}{L^3}$. Length scaling was usually taken to be the average of semimajor axes of the initial and final orbits, and time scaling was set either to 1 (no scaling) or one orbital period of an orbit with semimajor axis equal to the length scaling factor.

4.1.3.2 Drag smoothing

The US Standard Atmosphere model introduced in Section 2.2.2.2 is defined piecewise, wich is not compatible with Ipopt. A smooth reformulation is therefore needed. This will be achieved in two steps.

Firstly, define the unit interval indicator function $\mathbb{I}(x)$ as

$$\mathbb{I}(x) = \begin{cases} 1, 0 \le x < 1 \\ 0, \text{ otherwise} \end{cases} \tag{4.4}$$

and rewrite the piecewise definition for $\rho(r)$ in Equation (2.24) as

$$\rho(r) = \sum_{i=1}^{28} \rho_i \exp\left(-\frac{(r - (h_i + R))}{H_i}\right)\mathbb{I}(\frac{r - R - h_i}{h_{i+1} - h_i}). \tag{4.5}$$

Secondly, define a smooth indicator function $\sigma_k(x)$ as

$$\sigma_k(x) = \frac{1}{2}\left(\tanh kx + \tanh k(1-x)\right) \tag{4.6}$$

for some (large) value of $k > 0$. Then, the smooth density model $\rho_s(r)$ can be written

$$\rho(r) = \sum_{i=1}^{28} \rho_i \exp\left(-\frac{(r - (h_i + R))}{H_i}\right)\sigma_k\left(\frac{r - R - h_i}{h_{i+1} - h_i}\right), \tag{4.7}$$

thus giving an approximate, twice differentiable model as desired. With $k = 200$,

$$\max_r \frac{|\rho(r) - \rho_s(r)|}{\rho(r)} \leq 2\%, \tag{4.8}$$

which was deemed an acceptable approximation error.

4.1.4   Primer vector algorithm

The primer vector calculation methods from Sections 2.4.1.1 and 2.4.2.1 apply only between two consecutive impulses. Figure 4.2 shows a diagram with the algorithm for a general maneuver. First, the primer vector trajectory between all pairs of consecutive impulses is calculated. Then, if the maneuver starts with a coasting arc, the primer vector is propagated backwards with its transition matrix. Similarly, for the last impulse, the primer vector is propagated forwards.

Thereafter, the primer vector trajectory is analyzed. By construction, $\mathbf{p}$ should be continuous, and $\mathbf{p} = \hat{\mathbf{u}}$. What is left to verify is whether $\dot{\mathbf{p}}$ is continuous and $\|\mathbf{p}\| \leq 1$ during the maneuver.
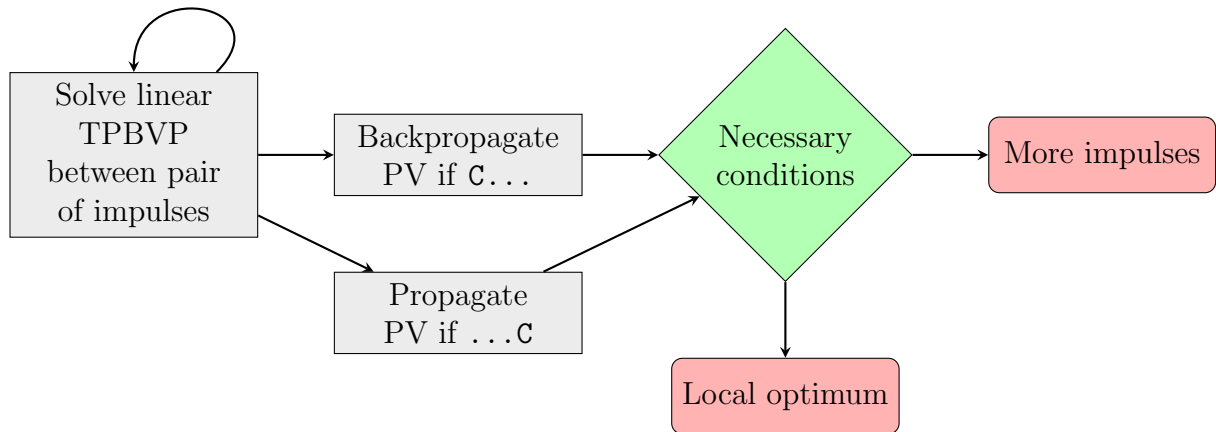

FIGURE 4.2 – Primer vector trajectory calculation algorithm, and conclusions that may be drawn from their analysis.

4.2 Primer vector meta-algorithm

Finally, with all of those components in place, an algorithm based on Luo *et al.* (2010) was implemented, and is represented in Figure 4.3. First, a case with fixed time impulses, `ICI`, analogous to a Lambert problem (TODO keep or not?) is solved. Usually, this gives a local optimum with very high cost. Then, initial and final coasts are added, and the primer vector trajectory is analyzed. If the primer vector norm exceeds 1, an impulse is added and the algorithm is repeated. If the continuity of the primer vector's derivative is violated, more random guesses are executed until a continuous primer vector derivative trajectory is found. And finally, when all necessary conditions are met, the algorithm ends and returns a multiple-impulse local optimum.
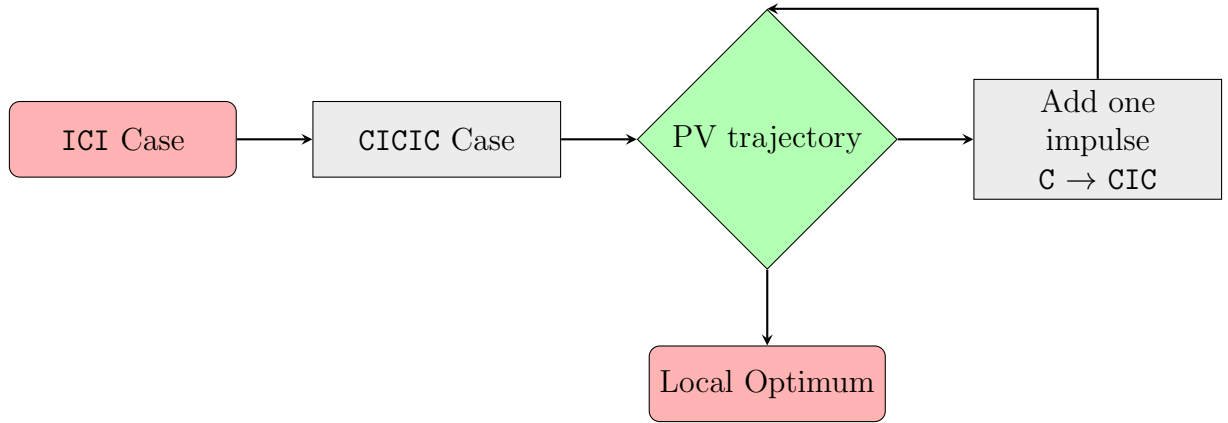
FIGURE 4.3 – Meta-algorithm with optimization and primer vector analysis.

5 Results

6 Conclusion

Bibliography

AERONAUTICS, N.; ADMINISTRATION, S. **Process for Limiting Orbital Debris**. [*S.l.*], 2021.

ANDERSSON, J. A. E.; GILLIS, J.; HORN, G.; RAWLINGS, J. B.; DIEHL, M. CasADi – A software framework for nonlinear optimization and optimal control. **Mathematical Programming Computation**, Springer, v. 11, n. 1, p. 1–36, 2019.

ARYA, V.; SALOGLU, K.; TAHERI, E.; JUNKINS, J. L. Generation of multiple-revolution many-impulse optimal spacecraft maneuvers. **Journal of Spacecraft and Rockets**, v. 60, n. 6, p. 1699–1711, 2023. Available at: https://doi.org/10.2514/1.A35638.

BERTSEKAS, D. P. **Dynamic Programming and Optimal Control Vol. I**. 1st. ed. [*S.l.*]: Athena Scientific, 1995. ISBN 1886529124.

BOKELMANN, K.; RUSSELL, R. Optimization of impulsive europa capture trajectories using primer vector theory. **The Journal of the Astronautical Sciences**, v. 67, 05 2019.

BRYSON, A. E.; HO, Y.-C. **Applied Optimal Control**. [*S.l.*]: Blaisdell Publishing Company, 1975.

CHAGAS, R. A. J.; CHAMBERLIN, T.; EICHHORN, H.; GAGNON, Y. L.; MENGALI, A.; BINZ, C.; SHOJI, Y.; STRA, F.; GASDIA, F.; YAMAZOE, H.; TAGBOT, J.; SRIKUMAR; CHENYONGZHI; JUSTBYOO. **JuliaSpace/SatelliteToolbox.jl: v1.0.0**. Zenodo, jan. 2025. Available at: https://doi.org/10.5281/zenodo.14586111.

CHOBOTOV, V. A. **Orbital Mechanics Third Edition**. [*S.l.*]: American Institute of Aeronautics and Astronautics, Inc., 2002.

CONWAY, B. **Spacecraft Trajectory Optimization**. [*S.l.*]: Cambridge University Press, 2010. (Cambridge Aerospace Series).

CURTIS, H. **Orbital Mechanics: For Engineering Students**. [*S.l.*]: Butterworth-Heinemann, 2020. (Aerospace Engineering).

FRANCO, T.; SANTOS, W. Gomes dos. Itasat-2: Formation flying maneuver and control considering j2 disturbances and differential drag. *In*: . **Proceedings** [...]. [*S.l.: s.n.*], 2020.

GLANDORF, D. R. Lagrange multipliers and the state transition matrix for coasting arcs. **AIAA Journal**, v. 7, n. 2, p. 363–365, 1969. Available at: https://doi.org/10.2514/3.5109.

JEZEWSKI, D. J.; ROZENDAAL, H. L. An efficient method for calculating optimal free-space n-impulse trajectories. **AIAA Journal**, v. 6, n. 11, p. 2160–2165, 1968. Available at: https://doi.org/10.2514/3.4949.

LASSERRE, J. B. **Moments, Positive Polynomials and Their Applications**. IMPERIAL COLLEGE PRESS, 2009. Available at: https://www.worldscientific.com/doi/abs/10.1142/p665.

LEANDER, R.; LENHART, S.; PROTOPOPESCU, V. Optimal control of continuous systems with impulse controls. **Optimal Control Applications and Methods**, v. 36, n. 4, p. 535–549, 2015. Available at: https://onlinelibrary-wiley-com.gorgone.univ-toulouse.fr/doi/abs/10.1002/oca.2128.

LION, P. M.; HANDELSMAN, M. Primer vector on fixed-time impulsive trajectories. **AIAA Journal**, v. 6, n. 1, p. 127–132, 1968. Available at: https://doi.org/10.2514/3.4452.

LUO, Y.-Z.; ZHANG, J.; LI, H. yang; TANG, G.-J. Interactive optimization approach for optimal impulsive rendezvous using primer vector and evolutionary algorithms. **Acta Astronautica**, v. 67, n. 3, p. 396–405, 2010. ISSN 0094-5765. Available at: https://www.sciencedirect.com/science/article/pii/S0094576510000652.

MONTENBRUCK, O.; GILL, E. **Satellite Orbits: Models, Methods, and Applications**. Springer Berlin Heidelberg, 2000. (Physics and astronomy online library). ISBN 9783540672807. Available at: https://books.google.fr/books?id=hABRnDlDkyQC.

MORELLI, A.; GIORDANO, C.; BONALLI, R.; TOPPUTO, F. Characterization of singular arcs in spacecraft trajectory optimization. 11 2023.

NASA. **ISS Environment**. 2009. Available at https://web.archive.org/web/20080213164432/http://pdlprod3.hosc.msfc.nasa.gov/D-aboutiss/D6.html.

PARADISO, R. **Soyuz MS-27 Reaches the ISS in Record Time – Here's How**. 2025. Available at https://www.spacevoyaging.com/news/2025/04/09/soyuz-ms-27-reaches-the-iss-in-record-time-heres-how/.

PRESS, W. H.; TEUKOLSKY, S. A.; VETTERLING, W. T.; FLANNERY, B. P. **Numerical Recipes 3rd Edition: The Art of Scientific Computing**. 3. ed. USA: Cambridge University Press, 2007. ISBN 0521880688.

PRUSSING, J. E.; CHIU, J.-H. Optimal multiple-impulse time-fixed rendezvous between circular orbits. **Journal of Guidance, Control, and Dynamics**, v. 9, n. 1, p. 17–22, 1986. Available at: https://doi.org/10.2514/3.20060.

ROSS, I. **A Primer on Pontryagin's Principle in Optimal Control**. Collegiate Publishers, 2015. ISBN 9780984357116. Available at: https://books.google.fr/books?id=KW5HrgEACAAJ.

SALOGLU, K.; TAHERI, E.; LANDAU, D. Existence of infinitely many optimal iso-impulse trajectories in two-body dynamics. **Journal of Guidance, Control, and Dynamics**, v. 46, n. 10, p. 1945–1962, 2023. Available at: https://doi.org/10.2514/1.G007409.

SATO, S.; COSTA, L.; MATOS, T.; JERONYMO, A.; MENEZES, R.; CASALE, D.; SCHUSTER, B.; VIEIRA, D. Itasat-2: Conops conops review and near-term challenges (ssc23-p4-25). p. 1, 08 2023.

SCHWARZ, R. **Memorandum No. 2: Cartesian State Vectors to Keplerian Orbit Elements**. 2014. Available at https://downloads.rene-schwarz.com/.

SUKHANOV, A. **Lectures on Atsrodynamics**. [*S.l.*]: INPE, 2010.

TAHERI, E.; JUNKINS, J. How many impulses redux. **The Journal of the Astronautical Sciences**, v. 67, 12 2019.

VERNER, J. Numerically optimal runge-kutta pairs with interpolants. **Numerical Algorithms**, v. 53, p. 383–396, 03 2010.

WäCHTER, A.; BIEGLER, L. On the implementation of an interior-point filter line-search algorithm for large-scale nonlinear programming. **Mathematical programming**, v. 106, p. 25–57, 03 2006.